Chinese Journal of
POLYMER SCIENCE

RESEARCH ARTICLE

https://doi.org/10.1007/s10118-023-3002-7
Chinese J. Polym. Sci. **2023**, *41*, 1937–1946

Robust and High-Wettability Pristine Poly(ether ether ketone) Nanofiber Separator for Heat-Resistant and Safe Lithium-Ion Battery

Xin-Ke Dai[a,b], Feng-Shan Yu[a,b], Jia-Wei Wen[a,b], Chun-Xia Wang[a,b], Xin-Long Ma[b], Wang Yang[b], Guo-Yong Huang[a,b*], and Hai-Mu Ye[a,b*]

[a] *College of New Energy and Materials, China University of Petroleum, Beijing 102249, China*
[b] *State Key Laboratory of Heavy Oil Processing, China University of Petroleum, Beijing 102249, China*

Electronic Supplementary Information

Abstract Separator is a pivotal component of lithium-ion batteries (LIBs) and determines the electrochemical performance and safety. However, with the increase in energy density and application scenarios, commercial polyolefin separators are increasingly unable to undertake heavy responsibility of battery safety protection. Herein, a new kind of nanofiber separator based on poly(ether ether ketone) (PEEK) with excellent thermal stability, self-extinguishing, and superior electrochemical properties is reported. Effective inheritance of intrinsic properties from raw PEEK materials and optimized hot-pressing operation endows the separator with high robustness and wettability, showing tensile strength of 15.8 MPa and a contact angle of 17.2°. The high thermal stability of PEEK can ensure the separator to preserve the structural integrity and microstructure at temperatures beyond 300 °C, and the excellent self-extinguishing peculiarity of PEEK capacitates the high safety of LIB. Notably, benefitting from high porosity and polar surface, the PEEK separator shows high electrolyte uptake of 245.5% and exhibits a wider electrochemical window and faster lithium-ion transport number than commercial polyolefin separators. Furthermore, cells assembled with PEEK separator display better performance than the ones with PE separator, and the PEEK LIB has been successfully used to light up a lamp at a high temperature of 150 °C.

Keywords Separator; Lithium-ion battery; Heat-resistance; PEEK

Citation: Dai, X. K.; Yu, F. S.; Wen, J. W.; Wang, C. X.; Ma, X. L.; Yang, W.; Huang, G. Y.; Ye, H. M. Robust and high-wettability pristine poly(ether ether ketone) nanofiber separator for heat-resistant and safe lithium-ion battery. *Chinese J. Polym. Sci.* **2023**, *41*, 1937–1946.

INTRODUCTION

Lithium-ion batteries (LIBs), the most widely used secondary batteries, have been controversial in recent years due to their safety problems.[1–5] As a constituent part of LIB, the separator located between the anode and cathode plays a crucial role in preventing internal short circuit and provides an electrolyte reservoir to enable ion transporting.[6–8] Therefore, the separator is essentially responsible for the safety of LIB. Until now, the most commonly used separators in LIBs are porous polyolefin membranes including polyethylene (PE) and polypropylene (PP), which have good physicochemical properties and suitable microstructure. However, the intrinsically low thermal deformation temperatures make them suffer from large shrinkage behavior and even serious breakage when heated. Consequently, a short circuit might happen and a large amount of heat would be generated inside LIB, which further causes accidents such as fire or explosion.[9] The continuous improvement of the energy density and expansion of application scenarios of LIBs require new types of separators with good heat-resistant performance beyond polyolefin separators, so the development of LIB separators has been a critical and challenging issue.[10–14]

Great effort has been exerted to improve the heat-resistance of LIB separators. The common solution is to incorporate inorganic nanofillers (such as Al_2O_3,[15] SiO_2,[16] TiO_2,[17] ZrO_2,[18] and ceramic[19]) onto/into polyolefin membranes, which has been commercialized. Nevertheless, the use of low thermal stable binders still affects the performance of LIBs at high temperatures.[20,21] In addition, the fall-off of nanofillers caused by swelling of the binder in the liquid electrolyte severely lessens the service life of battery.[22] Last but not least, adding inorganic particles might increase weight and deteriorate the mechanical strength of separators, which are not conducive to the augment of battery energy density and safety.[23] Besides the above-mentioned coating separators, fabrication of separator from high-temperature resistant materials, such as polyacrylonitrile (PAN),[24] poly(ethylene terephthalate) (PET),[25] poly(vinylidene fluoride) (PVDF),[26] and poly(vinyl alcohol) (PVA),[27] is another choice. Considering

* Corresponding authors, E-mail: huanggy@cup.edu.cn (G.Y.H.)
E-mail: yehaimu@cup.edu.cn (H.M.Y.)

Received March 3, 2023; Accepted May 11, 2023; Published online June 26, 2023

the key factors of separator including light-weight, stability and safety, engineering plastics, especially super engineering plastics with excellent mechanical strength, chemical stability, heat resistance and electrical insulation could be the optimal materials for separator.[28–32]

However, engineering plastics possess excellent chemical and thermal stability, which make it tricky to match suitable solvents for solution processing or directly prepare separator by molten process. Accordingly, the fabrication of engineering plastic separator usually needs specific modification to improve the solubility or indirect preparation path, which usually degrade the performance of engineering plastic separators and even the batteries. Liu *et al.* produced a polyformaldehyde (POM) separator by mixing POM with diluent (diphenylketone) at 180 °C, followed by a series of complex processes.[33] The POM separator showed obvious color change at 140 °C and a thermal shrinkage rate of 4.3% at 150 °C. The battery with the POM separator exhibited rapid discharge capacity decay and even short circuit. Zhang *et al.* used poly(amic acid) (PAA) as the precursor solution and fabricated the polyimide (PI) separator by nonsolvent-induced phase separation (NIPS).[34] The electrochemical impedance spectroscopy (EIS) test result of PI separator in Li-Li symmetric battery was as high as 1200 Ω corresponding to the low interfacial compatibility and high Li^+ migration resistance. Li *et al.* manufactured the polytetrafluoroethylene (PTFE) membrane by electrospinning and sintering.[35] However, the residual carbon and a small amount of poly(vinyl alcohol) (PVA) after separator sintering affected the performance of the assembled battery, and the capacity retention rate decreased to about 88.3% at 0.2 C after only 50 cycles. Li *et al.* chemically modified poly(ether ether ketone) (PEEK) to increase solubility and fabricated porous membrane by phase separation method.[36] The separator was in almost totally amorphous state and led to a thermal shrinkage rate as high as 18.3% at 246 °C. The PEEK separator fabricated by Liu *et al. via* thermal induced phase separation (TIPS) method showed obvious color changes at 150 °C and turned seriously yellow and black at 300 °C, which might be due to the existence of a large number of impurities such as diluent in separator.[37] Therefore, it is still urgent and challenging to fabricate separators suitable for LIBs from engineering plastics with the maximum intrinsic properties.

Here, PEEK as a typical super engineering plastic is selected to investigate the manufacture and characterization of the separator suitable for LIBs. The skeleton of PEEK consists of aromatic rings, which gives PEEK excellent mechanical properties, chemical stability, and thermal stability. In addition, abundant polar groups of the PEEK chain, such as ether bond and carbonyl group, make it have a good wettability for the electrolyte.[38,39] We previously realized the nanofabrication of PEEK through a strategy containing procedures of coaxial electrospinning and subsequent treatments of annealing at low temperatures and removal of the outer sheath, which furnishes a viable basis for the fabrication of engineering plastic mats (Fig. S1 in the electronic supplementary information, ESI).[40] As shown in Scheme 1, the electrospun PEEK nanofiber mat was further fabricated to separator by hot-pressing above the glass transition temperature (T_g), which could increase the crystallinity of PEEK nanofiber membranes and improve the mechanical strength to meet requirements of LIB separator. Then, the electrochemical performance and assembly battery of the PEEK separator were explored and evaluated.

EXPERIMENTAL

Materials

PEEK (G22) and poly(butylene succinate) (PBS, TH803S) were produced by Victrex Co., and Xinjiang Blue Ridge Tunhe Sci.&Tech. Co., Ltd., respectively. Dichloroformic acid (DCA) and hexafluoroisopropanol (HFIP) were purchased from Shanghai Aladdin Co. Commercial PE separator was produced by Asahi Kasei Co. Li chip, $LiFePO_4$ (D3), normal liquid electrolyte (KLD-LP02), and high voltage liquid electrolyte (KLD-5V02) for linear sweep voltammetry (LSV) test only were purchased from

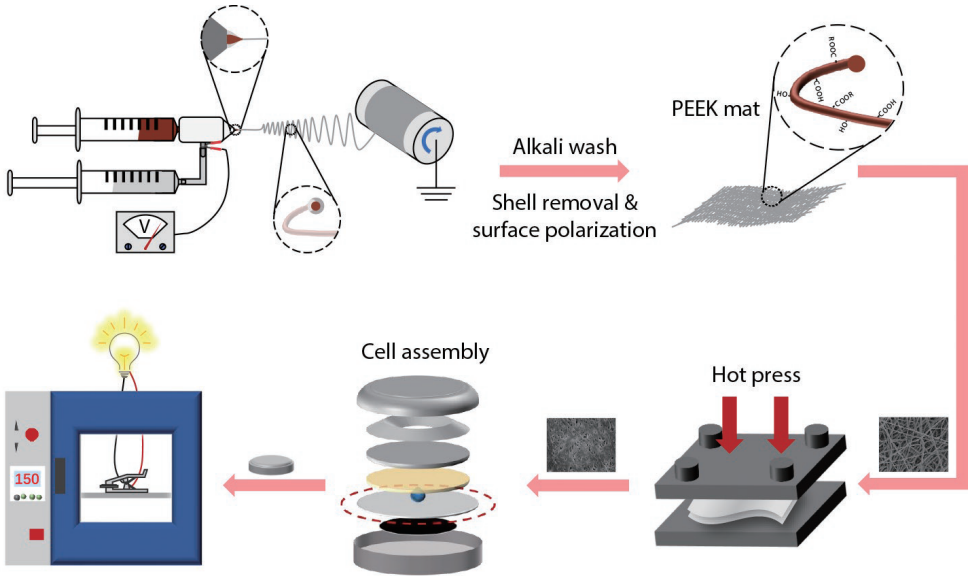

Scheme 1 Preparation of PEEK separator and assembly of the coin cell.

https://doi.org/10.1007/s10118-023-3002-7

Guangdong Canrd New Energy Technology Co., Ltd. A commercial high-temperature-resistant liquid electrolyte (LX-081, Fosai Chemicals®) was used as the working electrolyte for the high-temperature test.

Preparation of PEEK Nanofiber Membrane

PEEK was dissolved in DCA with a mass fraction of 9% by stirring at 185 °C for 1 h to get a homogeneous solution. PBS was added in HFIP with a mass fraction of 9% and stirred at room temperature for 5 h to obtain a uniform solution. Then, the PBS-coated PEEK (PBS@PEEK) nanofiber membrane was prepared through a coaxial electrospinning process with an electrospinning machine (HD-2313, Ucalery®). The optimal electrospinning parameters were chosen as follows:[40] the dimensions of the inner and outer needles were 0.26 and 0.90 mm, respectively. The pumping velocities of two kinds of solution in the inner (PEEK) and outer (PBS) needles were 0.20 and 0.53 mL/h, respectively. The voltage applied to the needle and the receiving roller was +24 and −2 kV, respectively. The collecting distance between the needle tip and the collector was 15 cm. The as-received PBS@PEEK nanofiber membrane was first stored at −10 °C for 48 h. Subsequently, the membrane was soaked in a 50 g/L KOH solution at 80 °C for 48 h to remove the PBS shell. Finally, the remaining PEEK nanofiber membrane was washed with exceed deionized water and dried in a vacuum oven at 80 °C for 24 h.

Fabrication of PEEK Separator and Cell

Two layers of PEEK nanofiber membranes with a thickness of 50 μm were stacked together and hot-pressed at 160 °C (slight above the T_g) and 16 MPa for 3 min in a plate vulcanizing machine (XLB, Qingdao Yahua®). Following by naturally cooling down to room temperature, the pressure was released and the sample was taken out and cut into circular PEEK separators with a diameter of 19 mm using a tablet press (MSK-T10, Shenzhen Kejing®).

$LiFePO_4$, acetylene black, and PVDF in *N*-methyl-2-pyrrolidinone (NMP) were mixed in a ratio of 8:1:1. The anode slurry was added with 1.5–2.0 g of NMP to achieve the proper flow state and stirred magnetically for 12 h. The slurry was coated on one side of the aluminum foil with a coating thickness of 100 μm using an automatic thick film coater (MSK-AFA-IIID, Hefei Kejing®) and dried in a vacuum oven at 80 °C 12 h. Then, the electrodes were punched into disks with a diameter of 12 mm using a tablet press (MSK-T10, Shenzhen Kejing®). The amount of $LiFePO_4$ in each disk was 1.0–1.5 mg (*i.e.*, 0.88–1.33 mg/cm^2). The coin cell was assembled in the order of anode can, positive electrode, 25 μL of electrolyte, separator, 25 μL of electrolyte, lithium chip, stainless steel spacer, stainless steel spring, and cathode cap. The assembled cell was sealed using a hydraulic crimping machine (MSK-110, Shenzhen Kejing®) with a pressure of 50 kg/cm^2. All processes were carried out in an argon-filled glove box (Super, Mikrouna®) where H_2O and O_2 content were less than 0.1 ppm.

Characterization

Wide angle X-ray diffraction (WAXD) characterization was performed on a multifunction diffractometer (DX-2700BH, Haoyuan®) with a scanning rate of 5 (°)/min in the range of 5°–60°. Fourier transform infrared (FTIR) spectra of raw PEEK and PEEK separator were recorded on an FTIR spectrometer (Tensor II, Bruker®) in a wavenumber range of 4000–650 cm^{-1}. The surface and cross-sectional micro-morphologies of the separator were observed using a scanning electron microscope (SEM, Quanta 200F, FEI®), and the cross-sectional samples were obtained by fracturing PEEK separators in liquid nitrogen. The mechanical properties were tested on a universal tensile machine (AGS-X, Shimadzu®) at a speed of 10 mm/min under room temperature. The sample size is 20 mm × 5 mm × 0.04 mm. The porosity of the separator was calculated by a soaked-in *n*-butanol method with Eq. (1):[41]

$$\text{Porosity}\ (\%) = \frac{(W - W_0)\,\rho}{\rho W + (\rho - \rho_0)W_0} \times 100\% \quad (1)$$

where W_0 and W represent the weight of the separator before and after soaking in *n*-butanol for 8 h, respectively; ρ and ρ_0 represent the density of separator material and *n*-butanol, respectively.

The thermal properties of samples were measured by a differential scanning calorimeter (DSC, 204F1, NETZSCH®) using dry nitrogen as protection and purge gas. The temperature range of the test was set between 25 and 200 °C with a heating rate of 5 °C/min. The thermal stability of PEEK separator was evaluated on a thermogravimetric analyzer (TGA, DTG-60, Shimadzu®) by heating the sample from 40 °C to 800 °C with a heating rate of 20 °C/min. The dimensional stability of samples regarding temperature was investigated by employing a parameter called thermal shrinkage rate (R_{ts}), which is figured out based on Eq. (2):

$$R_{ts}\,(\%) = \frac{S_0 - S}{S_0} \times 100\% \quad (2)$$

where S_0 and S are the values of separator area before and after thermal treating at the selected temperature for 1 h.

The contact angle between the electrolyte and the separator was tested by an optical contact angle & interface tension meter (SL200KS, KINO®) at room temperature under atmosphere, which help determine the wettability between the electrolyte and separator. The electrolyte uptake rate (R_{eu}) of the separator was obtained by soaking separator in the electrolyte for 8 h and then calculated by the rate of weight change according to Eq. (3):

$$R_{eu}\,(\%) = \frac{W_w - W_d}{W_d} \times 100\% \quad (3)$$

where W_d and W_w are the weights of the separator before and after soaking into the electrolyte, respectively.

LSV was used to measure the electrochemical window of the separator. The coin cell used in the LSV test was assembled by sandwiching the electrolyte-soaked separator between a Li chip and a stainless steel sheet and carried out from 3.0–5.5 V versus Li/Li$^+$ with a scan rate of 1 mV/s. AC impedance measurements were measured by sandwiching the electrolyte-soaked separator between two stainless steel sheets in a frequency range from 10^6 Hz to 1 Hz. The ionic conductivity of the separator was calculated according to Eq. (4):

$$\sigma = \frac{d}{S \times (R - R_0)} \quad (4)$$

where σ is the ionic conductivity; d is the thickness of the separator; S is the effective area of the separator; R is the

impedance of the separator; R_0 is the resistance of the coin cell shell and the electrodes tested by multimeter, which was set as the blank sample.

The lithium-ion transport number (t_{Li^+}) was tested by combining the chronoamperometry (CA) and EIS of the assembled Li/electrolyte-soaked separator/Li cells and calculated with Eq. (5):

$$t_{Li^+} = \frac{I_s \times (\Delta V - I_0 \times R_0)}{I_0 \times (\Delta V - I_s \times R_s)} \quad (5)$$

where I_0 and I_s are the initial and steady-state currents measured by CA, respectively; R_0 and R_s are the initial and steady-state resistances obtained by the EIS test, respectively; ΔV is the step potential difference (10 mV). The tests of LSV, CA and EIS were all performed on an electrochemical workstation (CHI 760E, CH Instruments®).

The cycle performance and rate performance of the cells were tested by CT2001A cell test instrument (LAND Electronic Co., Ltd., China) in the voltage range of 2.5–4.2 V.

RESULTS AND DISCUSSION

Microstructure and Wettability of PEEK Separator

The PEEK separator was constructed with stacking electrospun nanofibers, which provided good porosity and pore structure. Fig. 1(a) shows the SEM microstructure separator, in which nanofibers were well contacted with each other after being hot-pressed at 160 °C. Meanwhile, the structural feature of fibers was hardly affected. Such microstructure would benefit the balance between the mechanical properties of separator and the conduction of Li^+. For comparison, the microstructure of PE separator produced by a wet process is presented in Fig. 1(b), which displayed poor porosity and small pore size. In addition, the cross-section of PEEK separator (Fig. 1c) was much looser than the PE separator (Fig. 1d), which could be in favor of the rapid transport of Li^+. The multilayer dense structure in PE separator would bring greater resistance to the shuttle back and forth between the positive and negative electrodes of Li^+ during the charging and discharging process of the cell.[42,43]

The physical and chemical properties of PEEK separator and PE separator are tabulated in Table 1. The porosity of the PEEK separator was obviously higher than that of PE separator, 71.2% versus 40.0%. In principle, for a certain electrolyte, a separator with high porosity could help reduce impedance of the cell. However, extraordinarily high porosity would deteriorate the mechanical strength of the separator, and thus possibly induces many problems including penetration probability of lithium dendrite and self-discharge of the battery. Generally, separators prepared through the electrospinning method contain excessively high porosity and lead to poor mechanical performance. For example, the electrospun PVDF separator showed a porosity of up to 84.1% but only displayed tensile strength of 3.2 MPa and Young's modulus of 38.9 MPa.[44] The electrospun sulfonated PEEK (SPEEK) membrane (with 83.3% sulfonation degree) exhibited tensile strength of ~4.1 MPa.[45] Here, the tensile strength of PEEK separator increased from 11.4 MPa to 15.8 MPa (Fig. S2 in ESI) after hot-pressing, which were much higher than the reported electrospun separators.[46–50] The obvious promotion of mechanical properties could be ascribed to the hot-processing, which moderately reduced the porosity and enhanced the inter-fiber adhesion.

The high porosity of PEEK separator led to an excellent electrolyte uptake rate at as high as 245.5%, which was about 2.7 times higher than PE separator of 90.0% and remarkably higher than some of as-reported or as-claimed PEEK-relevant separators.[36,51,52] In addition, the molecular structure and the alkali washing process could make PEEK fiber getting higher polar surface property than PE. Consequently, the PEEK separator exhibits a much smaller contact angle (17.2°) for electrolytes than the PE separator (46.0°), as indicated in Fig. 2. The higher electrolyte uptake rate and lower contact angle of the PEEK separator for electrolytes reveal that PEEK separator has strong adsorption capacity to the electrolyte, facilitating rapid infiltration and storage of electrolyte and thus providing support for good performance of the cell.

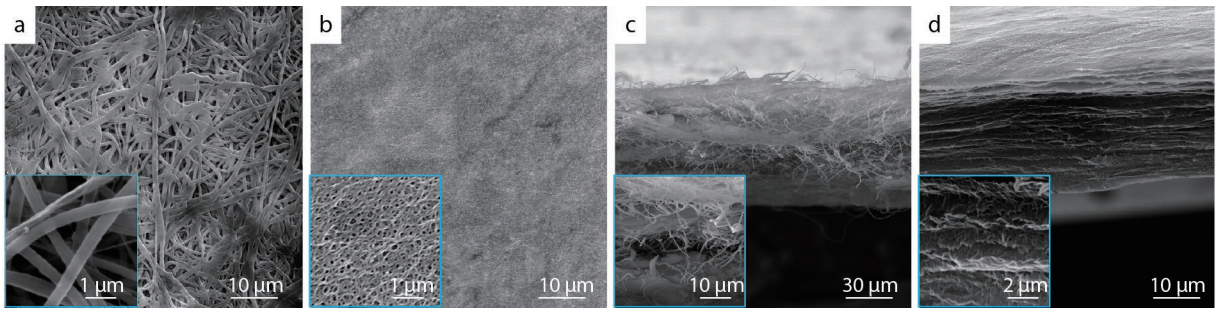

Fig. 1 Microstructure images of the (a) surface and (c) cross-section of the PEEK separator and the (b) surface and (d) cross-section of the commercial PE separator.

Table 1 Comparison of physical and chemical properties between PEEK separator and PE separator.

Separator	Thickness (μm)	Porosity (%)	Electrolyte uptake (%)	Ionic conductive (mS·cm^{-1})	Li^+ transport number	McMullin number [a] (N_M)	Tortuosity [b] (τ)
PEEK	40	71.2±6.9	245.5±49.4	1.48	0.425	7.66	2.335
PE	25	40.0±5.0	90.0±28.5	0.28	0.198	40.50	4.025

[a] $N_M = \sigma_o/\sigma_s$, where σ_o is the ionic conductivity of liquid electrolyte. The value is 11.34 mS·cm^{-1} here for 1 mol/L $LiPF_6$ in EC/DMC=1/1 (*V*/*V*). σ_s is the ionic conductivity of liquid electrolyte-filled separator. [b] $\tau = (N_M \times \varepsilon)^{1/2}$, where ε is the porosity of separator.

https://doi.org/10.1007/s10118-023-3002-7

Thermal Stability and Self-extinguishing Performance

As shown in Fig. 3(a), the as-fabricated PEEK separator did not show obvious shape change even at 300 °C, while the thermal shrinkage of PE separator is rather serious, severely crimping at 150 °C. From the thermal shrinkage curves in Fig. S3 (in ESI), PEEK separator only presented a thermal shrinkage of 3.4% at 300 °C, at which temperature PE separator had already melted seriously and turned black. The thermal stability of PEEK separator here was much higher than those of many reported PEEK-relevant separators (Table S1 in ESI). For instance, the PEEK separator prepared with sulfuric acid and methanesulfonic acid as the mixed solvent by NIPS method showed a thermal shrinkage rate as high as 37.7% at 150 °C,[53] where the PEEK chains had been seriously sulfonated. The excellent thermal stability of PEEK separator in this study should be attributed to the effective inheritance of physical properties of nanofiber membrane from the bulk. The chains were not chemically modified during separator preparation process, which retained the original excellent performance of raw PEEK to the maximum extent. X-ray diffractogram shown in Fig. S4 (in ESI) and FTIR

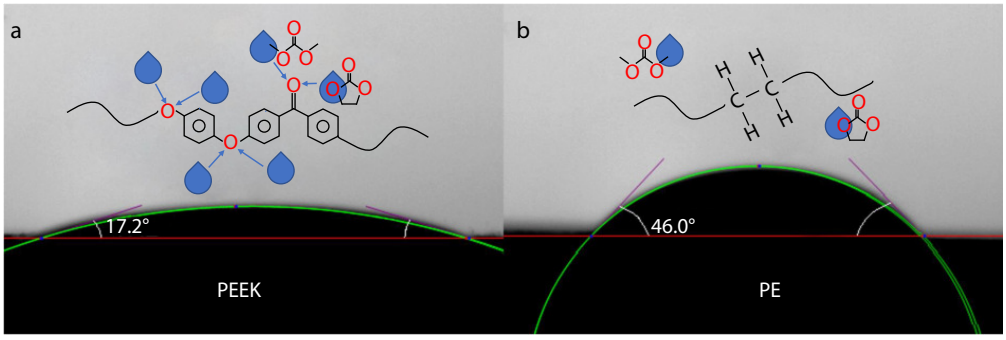

Fig. 2 Contact angles for electrolytes on the surface of (a) PEEK separator and (b) PE separator.

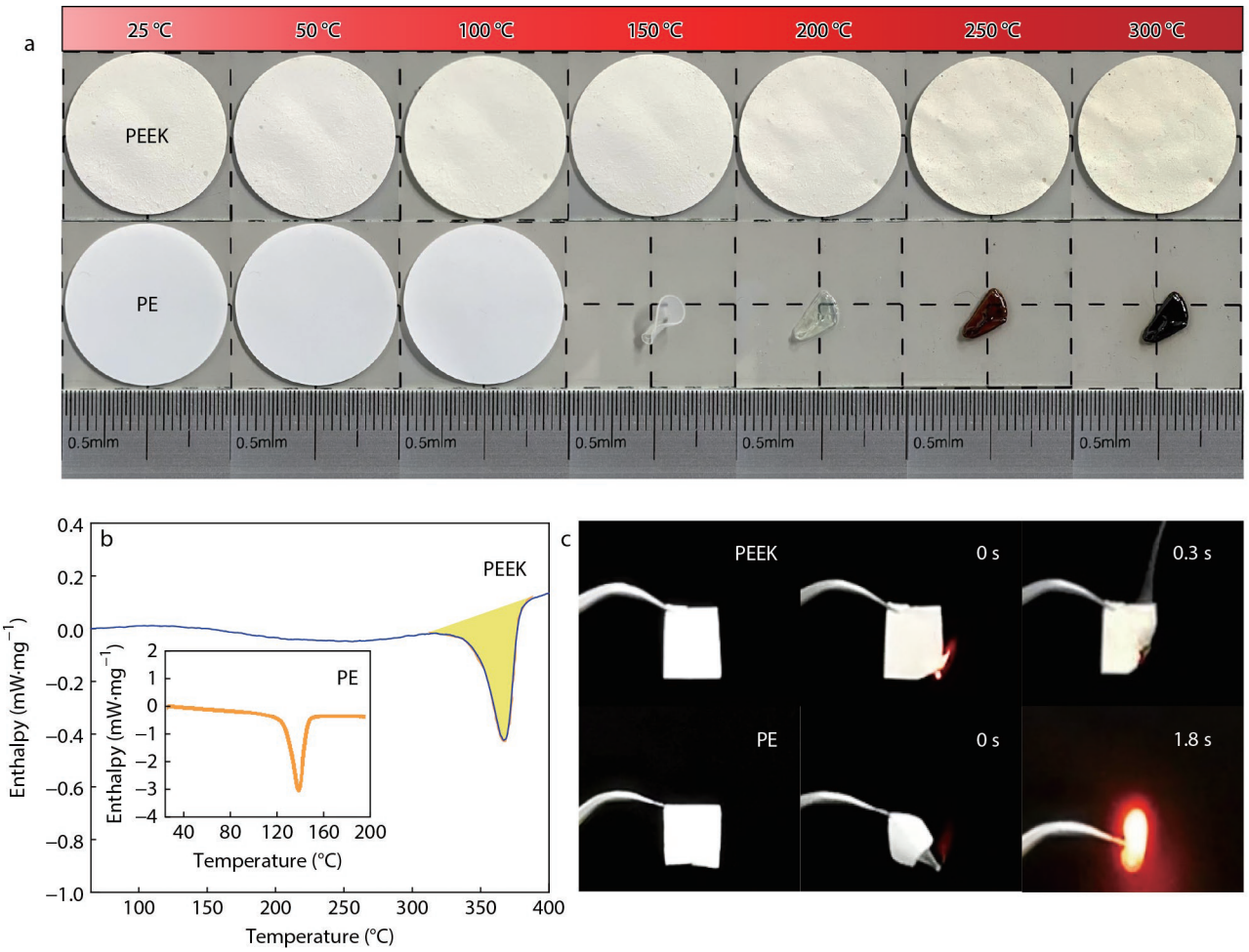

Fig. 3 (a) Photographs of PEEK separators and PE separators after being treated at different temperatures; (b) DSC heating curves of PEEK separator and PE separator; (c) Photographs of ignition test of PEEK separator and PE separator.

https://doi.org/10.1007/s10118-023-3002-7

spectra depicted in Fig. S5 (in ESI) confirmed the unchanged structure of PEEK and the absence of impurity.

The poor heat resistance of PE separator was not only related to the properties of material itself but also associated with fabricating process. PE separator suffered a stretching process during fabrication, which made it store remarkable internal stress, and led to significant shrinkage when the residual internal stress was released during heating. While, the PEEK fiber prepared by coaxial electrospinning was fully solution-crystallized inside the outer shell, where no internal stress could be induced.

It can be seen from the DSC curves in Fig. 3(b) that the PEEK separator showed a melting point as high as 367 °C, which was close to that of the raw PEEK (Fig. S6 in ESI). However, the PE separator just displayed a sharp exothermic peak at about 140 °C, demonstrating that the operating temperature of PE separator should be lower than 140 °C. In addition, the strong heat release during the melting process of PE separator would aggravate the thermal escape of lithium ions. In comparison with the un-hot-pressed mat,[39] PEEK separator possessed higher melting temperature (367 °C versus 364 °C) and crystallinity (47.1% versus 41.1%). Hot-pressing process at a temperature above T_g improved the thermal performance of PEEK separator. Furthermore, the self-extinguishing performance of separator was investigated. Both PEEK separator and PE separator were ignited by a lighter, as shown in Fig. 3(c). When the PE separator was moved toward the fire, it severely curled by heat and almost completely burned out after being ignited for 1.8 s. Differently, when the PEEK separator was put to the fire, it could maintain a good shape, and the self-extinguishing behavior finished within 0.3 s. The good thermal stability and self-extinguishing performance of PEEK separator provided safer opportunity for LIBs.

Electrochemical Characterization

As shown in Fig. 4(a), the maximum stable voltage of the system of PEEK separator and electrolyte determined from the LSV curve is 4.7 V, which is 0.6 V higher than that of PE separator system. So, PEEK separator could meet the operating conditions of most LIBs. The higher electrochemical stability of PEEK separator revealed the good performance inheritance from raw PEEK. According to Nyquist plots in Fig. 4(b), the calculated ionic conductivity of the system of PEEK separator and electrolyte is 1.48 mS·cm^{-1}, which is 5.3 times higher than that of the PE separator system (0.28 mS·cm^{-1}) and 2.1 times higher than that of the lithiated PEEK separator system *via* lithiation of PEEK and TIPS method below the melting point.[51] The high ionic conductivity value originated from the good wettability of PEEK separator with polar electrolytes, which facilitated the movement of ions in electrolytes.

However, the ionic conductivity of a cell is composed of anions and cations. In other words, high ionic conductivity does not necessarily and directly reveal the high transport efficiency of Li^+. Hence, the Li^+ transport number was further used to evaluate the transport efficiency of Li^+. The CA test curves are presented in Fig. 5(a). The initial and stable currents of PEEK separator system are all higher than those of the PE separator system, indicating a lower impedance in PEEK system, which can also be found from the impedances of the PEEK separator system before and after polarization in Fig. 5(b). The lower impedance value of the Li symmetrical cell manifested that PEEK separator has better interfacial compatibility with the Li electrode than the PE separator, which benefited the rapid transport and uniformed deposition of Li^+. The Li^+ transport number of the PEEK separator system was 0.425, which was more than twice of PE separator system (*i.e.*, 0.198). Therefore, when PEEK separator was used instead of PE separator, the transport efficiency of Li^+ could be obviously promoted. The polar surface of the PEEK chain benefited interaction between separator and electrolytes, which would weaken the solvation of Li^+. As a result, more Li^+ could migrated less constrainedly, and thus, the Li^+ transport number increased.

Cell Performance

As presented above, it is expected that PEEK LIBs would perform better than PE LIBs. So, the cycle performance of the cell was investigated. As shown in Fig. 6(a), the initial discharge specific capacity of the cell with PEEK separator is 127.6 mAh·g^{-1} at a rate of 1 C. The capacity gradually decreases to 100.9 mAh·g^{-1} after 150 cycles. The capacity retention rate was 79.1%. For comparison, the initial discharge specific capacity of the cell with PE separator was just 115.0 mAh·g^{-1} under 1 C condition, and the value declines to 90.8 mAh·g^{-1} after 150 cycles,

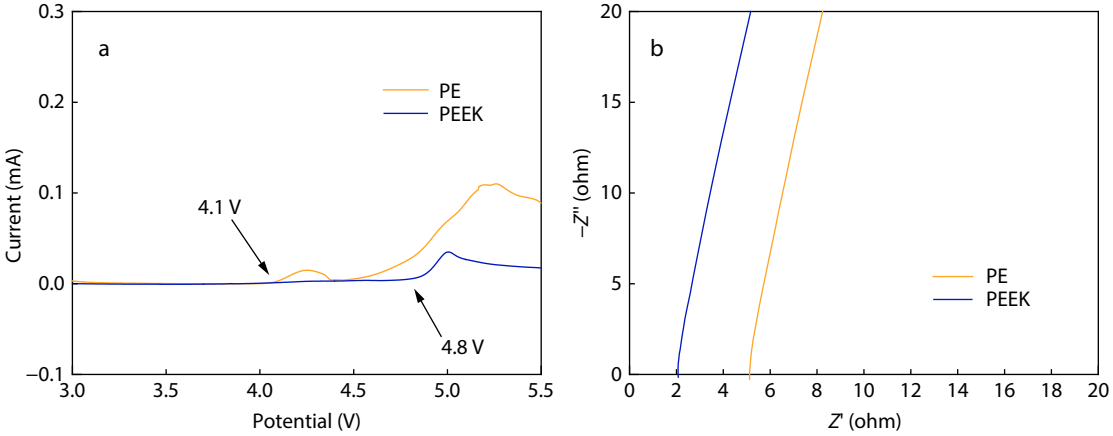

Fig. 4 (a) LSV curves and (b) the Nyquist plots of the PEEK separator and PE separator.

https://doi.org/10.1007/s10118-023-3002-7

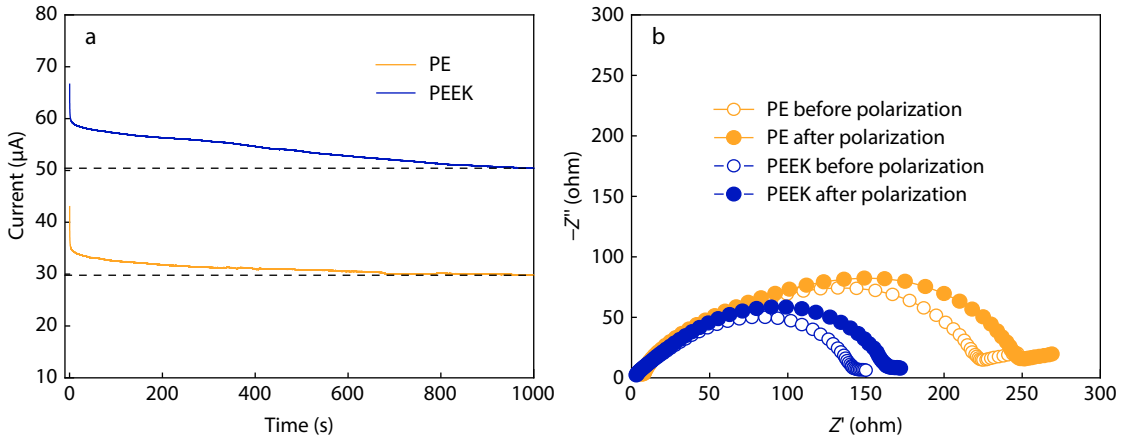

Fig. 5 (a) The CA test curves of the PEEK separator and PE separator; (b) The impedance curves before and after polarization.

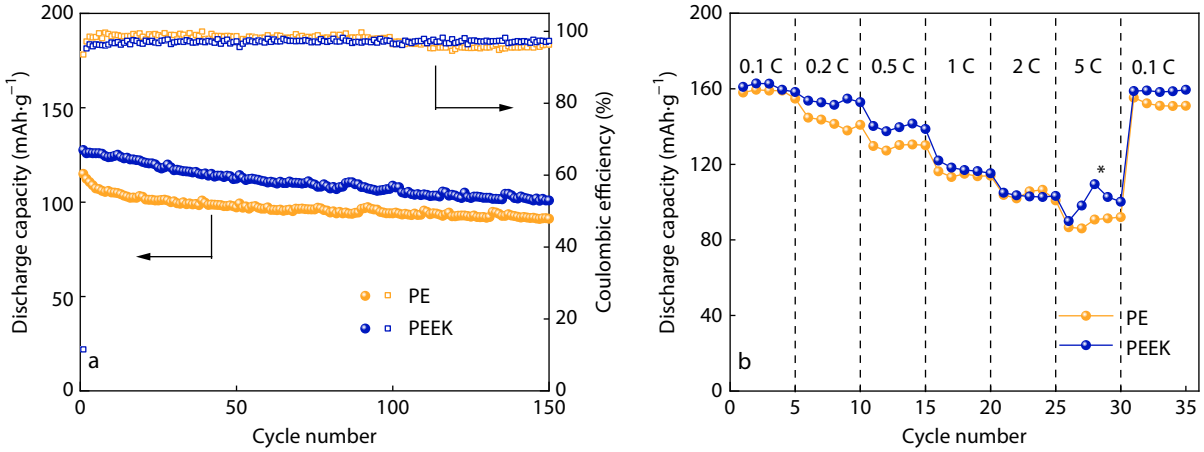

Fig. 6 (a) The cycle performance and (b) the rate performance of batteries with PEEK separator and PE separator. * There was a period of current vanishing caused by the test system during charging process of the third cycle at 5 C rate, which led to an abnormal jump of data.

equaling a capacity retention rate of 79.0%. The cell with the PE separator shows a rapid drop in the first 20 cycles, which might be due to the interface impedance problem caused by the weak polarity of PE separator, while the PEEK cell exhibited a smoother process. Moreover, the Coulombic efficiency of the cell with PEEK separator in Fig. 6(a) shows an upward trend in 150 cycles, but that of PE separator displays a downward trend. The Coulombic efficiency of PEEK cell at the 150th cycle was 97.4%, which was higher than that of PE cell (96.3%). Therefore, the cell with PEEK separator exhibited better cycle performance than that with PE separator.

Furthermore, the discharge behaviors of cells at different rates from 0.1 C to 5 C were systematically studied. The initial discharge curves of cells with PEEK separator and PE separator are shown in Fig. S7 (in ESI). Inspiringly, the initial discharge specific capacity of PEEK cell was always higher than the PE cell under each discharge condition, that is, 161.0 mAh·g^{-1} versus 158.0 mAh·g^{-1} at 0.1 C, 153.7 mAh·g^{-1} versus 144.7 mAh·g^{-1} at 0.2 C, 140.3 mAh·g^{-1} versus 129.7 mAh·g^{-1} at 0.5 C, 122.0 mAh·g^{-1} versus 116.3 mAh·g^{-1} at 1 C, 105.0 mAh·g^{-1} versus 103.8 mAh·g^{-1} at 2 C, and 90.0 mAh·g^{-1} versus 86.7 mAh·g^{-1} at 5 C. The discharge specific capacities and the capacity retentions of PEEK cell were basically higher than that of PE cell at each all rate, except sometimes at 2 C rate (Fig. 6b). After cycling at various rates, the PEEK cell exhibits a good capacity retention of 99.1% at 0.1 C rate in comparison with 95.6% for PE cell. The better high-rate performance of cells with PEEK separators was primarily due to the excellent porosity and wettability of the electrolyte, which enabled rapid Li^+ transport. Moreover, the good interface compatibility between the PEEK separator and lithium anode made Li^+ suffer small interface impedance during transport, which was conducive to the rapid charging and discharging of cells.

To explore the high-temperature performance of cell with PEEK separator, the assembled cell with commercial high-temperature-resistant liquid electrolyte was first cycled 3 cycles at 0.1 C rate and room temperature to ensure the normal cell conditions before subjecting to high-temperature measurements. Afterward, the cell was placed at 150 °C for 1 h and tested with cycle performance at a charge-discharge rate of 0.1 C after naturally cooling down to room temperature. Fig. 7(a) illustrates the cycle performance after 150 °C treatment. The PE cell lost its performance at room temperature after thermal treatment, which could be due to the melting and closed pores of the PE separator (Fig. S8a in ESI). The Li^+ transportation was blocked. However, the PEEK cell could still run relatively steadily after thermal treatment. The morphology of PEEK separator after experiencing the measure-

https://doi.org/10.1007/s10118-023-3002-7

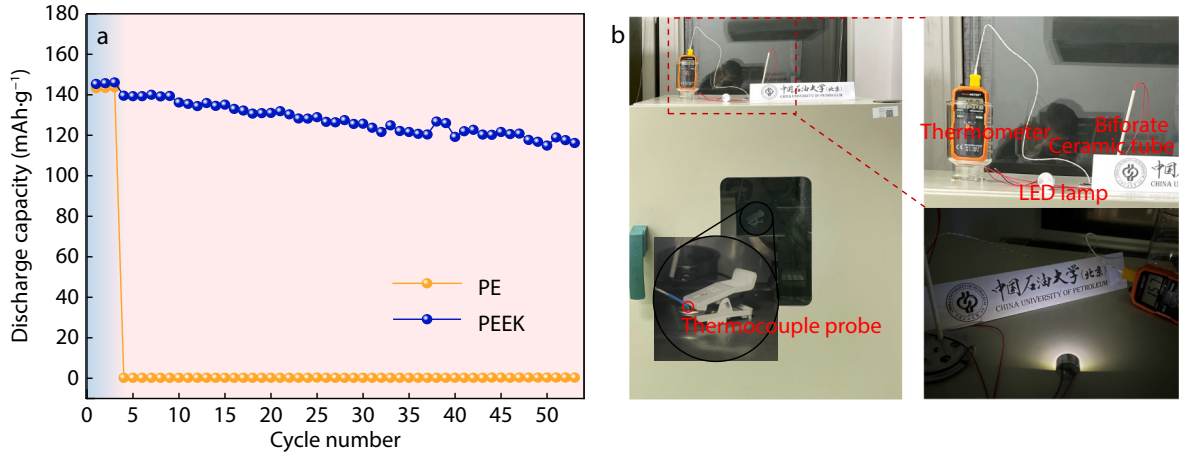

Fig. 7 (a) The cycle performance of cells with PE and PEEK separators before and after being placed at 150 °C for 1 h; (b) The images of the PEEK cell working at 150 °C (set value, with a detected value of 157 °C).

ment process of Fig. 7(a) is shown in Fig. S8b (in ESI). The microstructure of PEEK separator kept almost unchanged, which guaranteed the cell performance. To confirm the availability of cell with PEEK separator working at high temperature, the cell was used to light up a 3 W LED lamp at 150 °C (Fig. 7b), demonstrating the distinguished thermal stability of the PEEK separator and the great potential for its application in high-temperature-related scenes, such as oil and gas exploration, aerospace and aviation. Therefore, the PEEK separator with high-temperature resistance and good surface structure is a promising candidate for LIBs working at high temperatures. Certainly, the PEEK separator could be expected to work at temperatures much higher than 150 °C by referring to its thermal properties and shape stability, when electrolytes with higher boiling points could be involved.

CONCLUSIONS

In this work, we fabricated a pristine separator of PEEK with excellent thermal stability, self-extinguishing, and superior electrochemical properties, which displayed high porosity of 71.2% and tensile strength of 15.8 MPa. Meanwhile, it exhibited good wettability with a contact angle of 17.2° and electrolyte uptake of 245.5%, resulting in conspicuous ionic conductivity (1.48 mS·cm^{-1}) and a Li^+ transport number (0.425). The cell with the PEEK separator revealed an initial discharge specific capacity of 127.6 mAh·g^{-1} at 1 C and remains 79.1% of them after 150 cycles. In addition, the PEEK cell was further used to light up a 3 W LED lamp at 150 °C, indicating a promising application in advanced LIBs. Considering that the as-prepared PEEK separator owns thermal stability of up to 300 °C, the operating temperature of cells with PEEK separator could be further enhanced if a non-liquid electrolyte is used, which would broaden the application scenario of lithium secondary battery limited by temperatures, such as oil and gas exploration.

Conflict of Interests

The authors declare no interest conflict.

Electronic Supplementary Information

Electronic supplementary information (ESI) is available free of charge in the online version of this article at http://doi.org/10.1007/s10118-023-3002-7.

ACKNOWLEDGMENTS

This work was financially supported by the National Natural Science Foundation of China (Nos. 52022109, 51834008 and 22008248), Beijing Municipal Natural Science Foundation (No. 2202047), National Key Research and Development Program of China (No. 2021YFC2901100) and Science Foundation of China University of Petroleum, Beijing (Nos. 2462020YXZZ019, 2462021QNX2010, 2462020YXZZ016 and 2462022QZDX008).

REFERENCES

1 Liu, J.; Bao, Z. N.; Cui, Y.; Dufek, E. J.; Goodenough, J. B.; Khalifah, P.; Li, Q. Y.; Liaw, B. Y.; Liu, P.; Manthiram, A.; Meng, Y. S.; Subramanian, V. R.; Toney, M. F.; Viswanathan, V. V.; Whittingham, M. S.; Xiao, J.; Xu, W.; Yang, J. H.; Yang, X. Q.; Zhang, J. G. Pathways for practical high-energy long-cycling lithium metal batteries. *Nat. Energy* **2019**, *4*, 180–186.

2 Armand, M.; Tarascon, J. M. Building better batteries. *Nature* **2008**, *451*, 652–657.

3 Kim, T.; Song, W. T.; Son, D. Y.; Ono, L. K.; Qi, Y. B. Lithium-ion batteries: outlook on present, future, and hybridized technologies. *J. Mater. Chem. A* **2019**, *7*, 2942–2964.

4 Wu, F.; Maier, J.; Yu, Y. Guidelines and trends for next-generation rechargeable lithium and lithium-ion batteries. *Chem. Soc. Rev.* **2020**, *49*, 1569–1614.

5 Yang, Y.; Okonkwo, E. G.; Huang, G.; Xu, S.; Sun, W.; He, Y. On the sustainability of lithium ion battery industry—a review and perspective. *Energy Stor. Mater.* **2021**, *36*, 186–212.

6 Costa, C. M.; Lee, Y. H.; Kim, J. H.; Lee, S. Y.; Lanceros-Mendez, S. Recent advances on separator membranes for lithium-ion battery applications: from porous membranes to solid electrolytes. *Energy Stor. Mater.* **2019**, *22*, 346–375.

7 Arora, P.; Zhang, Z. M. Battery separators. *Chem. Rev.* **2004**, *104*, 4419–4462.

8 Wang, F.; Ke, X.; Shen, K.; Zhu, L.; Yuan, C. A critical review on materials and fabrications of thermally stable separators for lithium-ion batteries. *Adv. Mater. Technol.* **2022**, *7*, 2100772.
9 Loveridge, M.; Remy, G.; Kourra, N.; Genieser, R.; Barai, A.; Lain, M.; Guo, Y.; Amor-Segan, M.; Williams, M.; Amietszajew, T.; Ellis, M.; Bhagat, R.; Greenwood, D. Looking deeper into the galaxy (Note 7). *Batteries* **2018**, *4*, 3.
10 Heidari, A. A.; Mahdavi, H. Recent development of polyolefin-based microporous separators for Li-ion batteries: a review. *Chem. Rec.* **2020**, *20*, 570–595.
11 Rao, E.; McVerry, B.; Borenstein, A.; Anderson, M.; Jordan, R. S.; Kaner, R. B. Roll-to-roll functionalization of polyolefin separators for high-performance lithium-ion batteries. *ACS Appl. Energy Mater.* **2018**, *1*, 3292–3300.
12 Costa, C. M.; Lizundia, E.; Lanceros-Méndez, S. Polymers for advanced lithium-ion batteries: state of the art and future needs on polymers for the different battery components. *Progr. Energy Combust. Sci.* **2020**, *79*, 100846.
13 Chen, Y.; Kang, Y.; Zhao, Y.; Wang, L.; Liu, J.; Li, Y.; Liang, Z.; He, X.; Li, X.; Tavajohi, N.; Li, B. A review of lithium-ion battery safety concerns: the issues, strategies, and testing standards. *J. Energy Chem.* **2021**, *59*, 83–99.
14 Sun, P.; Bisschop, R.; Niu, H.; Huang, X. A review of battery fires in electric vehicles. *Fire Technol.* **2020**, *56*, 1361–1410.
15 Palanisamy, M.; Lin, K. W.; Lo, C. T.; Pol, V. G. *In situ* thermal safety aspect of the electrospun polyimide-Al_2O_3 separator reveals less exothermic heat energies than polypropylene at the thermal runaway event of lithium-ion batteries. *ACS Appl. Mater. Interfaces* **2022**, *14*, 28310–28320.
16 Fu, D.; Luan, B.; Argue, S.; Bureau, M. N.; Davidson, I. J. Nano SiO_2 particle formation and deposition on polypropylene separators for lithium-ion batteries. *J. Power Sources* **2012**, *206*, 325–333.
17 Chen, H.; Lin, Q.; Xu, Q.; Yang, Y.; Shao, Z. P.; Wang, Y. Plasma activation and atomic layer deposition of TiO_2 on polypropylene membranes for improved performances of lithium-ion batteries. *J. Membr. Sci.* **2014**, *458*, 217–224.
18 Zhu, X. M.; Jiang, X. Y.; Ai, X. P.; Yang, H. X.; Cao, Y. L. TiO_2 ceramic-grafted polyethylene separators for enhanced thermostability and electrochemical performance of lithium-ion batteries. *J. Membr. Sci.* **2016**, *504*, 97–103.
19 Raja, M. W.; Basu, R. N.; Pramanik, N. C.; Das, P. S.; Das, M. Paperator: the paper-based ceramic separator for lithium-ion batteries and the process scale-up strategy. *ACS Appl. Energy Mater.* **2022**, *5*, 5841–5854.
20 Dai, J.; Shi, C.; Li, C.; Shen, X.; Peng, L.; Wu, D.; Sun, D.; Zhang, P.; Zhao, J. A rational design of separator with substantially enhanced thermal features for lithium-ion batteries by the polydopamine-ceramic composite modification of polyolefin membranes. *Energy Environ. Sci.* **2016**, *9*, 3252–3261.
21 Yang, C.; Tong, H.; Luo, C.; Yuan, S.; Chen, G.; Yang, Y. Boehmite particle coating modified microporous polyethylene membrane: A promising separator for lithium ion batteries. *J. Power Sources* **2017**, *348*, 80–86.
22 Wang, M.; Chen, X.; Wang, H.; Wu, H.; Jin, X.; Huang, C. Improved performances of lithium-ion batteries with a separator based on inorganic fibers. *J. Mater. Chem. A* **2017**, *5*, 311–318.
23 Park, J. H.; Park, W.; Kim, J. H.; Ryoo, D.; Kim, H. S.; Jeong, Y. U.; Kim, D. W.; Lee, S. Y. Close-packed poly(methyl methacrylate) nanoparticle arrays-coated polyethylene separators for high-power lithium-ion polymer batteries. *J. Power Sources* **2011**, *196*, 7035–7038.
24 Cho, T. H.; Tanaka, M.; Onishi, H.; Kondo, Y.; Nakamura, T.; Yamazaki, H.; Tanase, S.; Sakai, T. Battery performances and thermal stability of polyacrylonitrile nano-fiber-based nonwoven separators for Li-ion battery. *J. Power Sources* **2008**, *181*, 155–160.
25 Hao, J. L.; Lei, G. T.; Li, Z. H.; Wu, L. J.; Xiao, Q. Z.; Wang, L. A novel polyethylene terephthalate nonwoven separator based on electrospinning technique for lithium ion battery. *J. Membr. Sci.* **2013**, *428*, 11–16.
26 Hwang, K.; Kwon, B.; Byun, H. Preparation of PVdF nanofiber membranes by electrospinning and their use as secondary battery separators. *J. Membr. Sci.* **2011**, *378*, 111–116.
27 Xiao, W.; Zhao, L.; Gong, Y.; Liu, J.; Yan, C. Preparation and performance of poly(vinyl alcohol) porous separator for lithium-ion batteries. *J. Membr. Sci.* **2015**, *487*, 221–228.
28 Luo, D.; Chen, M.; Xu, J.; Yin, X.; Wu, J.; Chen, S.; Wang, L.; Wang, H. Polyphenylene sulfide nonwoven-based composite separator with superior heat-resistance and flame retardancy for high power lithium ion battery. *Compos. Sci. Technol.* **2018**, *157*, 119–125.
29 Yanilmaz, M.; Dirican, M.; Zhang, X. W. Evaluation of electrospun SiO_2/nylon 6,6 nanofiber membranes as a thermally-stable separator for lithium-ion batteries. *Electrochim. Acta* **2014**, *133*, 501–508.
30 Huang, Z. H.; Chen, J. M.; Huo, Y. P.; Zhao, J. W. Heat resistant microporous membranes based on soluble poly(aryl ether ketone) copolymers for lithium ion battery separator. *J. Appl. Polym. Sci.* **2021**, *138*, e50895.
31 Liu, Y.; Ma, H.; Hsiao, B. S.; Chu, B.; Tsou, A. H. Improvement of meltdown temperature of lithium-ion battery separator using electrospun polyethersulfone membranes. *Polymer* **2016**, *107*, 163–169.
32 Li, D.; Shi, D.; Xia, Y.; Qiao, L.; Li, X.; Zhang, H. Superior thermally stable and nonflammable porous polybenzimidazole membrane with high wettability for high-power lithium-ion batteries. *ACS Appl. Mater. Interfaces* **2017**, *9*, 8742–8750.
33 Liu, J.; Yang, K.; Mo, Y.; Wang, S.; Han, D.; Xiao, M.; Meng, Y. Highly safe lithium-ion batteries: High strength separator from polyformaldehyde/cellulose nanofibers blend. *J. Power Sources* **2018**, *400*, 502–510.
34 Zhang, H.; Lin, C. E.; Zhou, M. Y.; John, A. E.; Zhu, B. K. High thermal resistance polyimide separators prepared *via* soluble precusor and non-solvent induced phase separation process for lithium ion batteries. *Electrochim. Acta* **2016**, *187*, 125–133.
35 Li, J.; Zhong, Q.; Yao, Y.; Bi, S.; Zhou, T.; Guo, X.; Wu, M.; Feng, T.; Xiang, R. Electrochemical performance and thermal stability of the electrospun PTFE nanofiber separator for lithium-ion batteries. *J. Appl. Polym. Sci.* **2018**, *135*, e46508.
36 Li, Z.; Cao, T. T.; Zhang, Y.; Han, Y.; Xu, S. M.; Xu, Z. H. Novel lithium ion battery separator based on hydroxymethyl functionalized poly(ether ether ketone). *J. Membr. Sci.* **2017**, *540*, 422–429.
37 Liu, J. C.; Mo, Y. D.; Wang, S. J.; Ren, S.; Han, D. M.; Xiao, M.; Sun, L. Y.; Meng, Y. Z. Ultrastrong and heat-resistant poly(ether ether ketone) separator for dendrite-proof and heat-resistant lithium-ion batteries. *ACS Appl. Energy Mater.* **2019**, *2*, 3886–3895.
38 Jones, D. P.; Leach, D. C.; Moore, D. R. Mechanical properties of poly(ether-ether-ketone) for engineering applications. *Polymer* **1985**, *26*, 1385–1393.
39 Lee, Y.; Porter, R. S. Double-melting behavior of poly(ether ether ketone). *Macromolecules* **1987**, *20*, 1336–1341.
40 Ye, H. M.; Zhu, W. Y.; Liu, P.; Wei, X.-W.; Li, H.; Cai, L.; Meng, X.; Huang, G.; Zhou, Q. Fabrication of shrinkage-free poly(ether ether ketone) nanofibrous mat and its use for flexible and thermally-recycled MOF composites. *Mater. Today Commun.* **2020**, *23*, 100862.
41 Dai, X.; Zhang, X.; Wen, J.; Wang, C.; Ma, X.; Yang, Y.; Huang, G.; Ye, H. M.; Xu, S. Research progress on high-temperature resistant polymer separators for lithium-ion batteries. *Energy Stor. Mater.* **2022**, *51*, 638–659.
42 Kim, P. J. Surface-functionalized separator for stable and reliable

https://doi.org/10.1007/s10118-023-3002-7

lithium metal batteries: a review. *Nanomaterials* **2021**, *11*, 2275.
43 Yang, Y. F.; Wang, W. K.; Meng, G. L.; Zhang, J. P. Function-directed design of battery separators based on microporous polyolefin membranes. *J. Mater. Chem. A* **2022**, *10*, 14137–11470.
44 Liang, Y.; Cheng, S.; Zhao, J.; Zhang, C.; Sun, S.; Zhou, N.; Qiu, Y.; Zhang, X. Heat treatment of electrospun polyvinylidene fluoride fibrous membrane separators for rechargeable lithium-ion batteries. *J. Power Sources* **2013**, *240*, 204–211.
45 Zhao, F.; Hu, S. H.; Wang, F. J.; Wang, L. A sulfonated PEEK/PCL composite nanofibrous membrane for periosteum tissue engineering application. *J. Mater. Sci.* **2019**, *54*, 12012–12023.
46 Xiao, W.; Song, J.; Huang, L.; Yang, Z. X.; Qiao, Q. D. PVA-ZrO_2 multilayer composite separator with enhanced electrolyte property and mechanical strength for lithium-ion batteries. *Ceram. Int.* **2020**, *46*, 29212–29221.
47 Dong, T.; Ul Arifeen, W.; Kim, M.; Choi, J.; Yoo, K.; Ko, T. J. Membranes made from electrospun polyacrylonitrile nonwoven fibers with uniform diameter for lithium-ion battery separators. *Fibers Polym.* **2020**, *21*, 2204–2214.
48 Khodaverdi, F.; Vaziri, A.; Javanbakht, M.; Jahanfar, M. Improvement of PAN separator properties using PVA/malonic acid by electrospinning in lithium ion-batteries. *J. Appl. Polym. Sci.* **2021**, *138*, e50088.
49 Cao, L. Y.; An, P.; Xu, Z. W.; Huang, J. F. Performance evaluation of electrospun polyimide non-woven separators for high power lithium-ion batteries. *J. Electroanal. Chem.* **2016**, *767*, 34–39.
50 Li, J.; Zhang, X.; Lu, Y.; Linghu, K.; Wang, C.; Ma, Z.; He, X. Electrospun fluorinated polyimide/polyvinylidene fluoride composite membranes with high thermal stability for lithium ion battery separator. *Adv. Fiber Mater.* **2022**, *4*, 108–118.
51 Li, L.; Xiong, R.; Wang, X.; Zhou, M.; Sun, S.; Shen, G.; Song, L.; Zhang, Y.; Zhou, H. Lithiated poly(ether ether ketone) separators with excellent thermal stability and electrolyte wettability for lithium-ion battery. *J. Mater. Sci.* **2022**, *57*, 18980–18992.
52 Li, Z.; Wang, W. Q.; Han, Y.; Zhang, L.; Li, S. S.; Tang, B.; Xu, S. M.; Xu, Z. H. Ether modified poly(ether ether ketone) nonwoven membrane with excellent wettability and stability as a lithium ion battery separator. *J. Power Sources* **2018**, *378*, 176–183.
53 Li, D.; Shi, D. Q.; Feng, K.; Li, X. F.; Zhang, H. M. Poly(ether ether ketone) (PEEK) porous membranes with super high thermal stability and high rate capability for lithium-ion batteries. *J. Membr. Sci.* **2017**, *530*, 125–131.

https://doi.org/10.1007/s10118-023-3002-7